

Supplementary Information

Reversal of Pancreatic Desmoplasia by Tumor Stromal Targeted Nitric Oxide Delivery Overcome

TRAIL resistance in Pancreatic Tumors

Method and Materials

Cells and materials:

Murine PDAC AK4.4 cells (KrasG12D and p53+/-) were kindly provided by Dr. Nabeel Bardeesy (Massachusetts General Hospital, Boston) and were isolated from mice with spontaneous pancreatic tumors (Ptf1-Cre/LSL-KrasG12D/p53Lox/+)[1]. Murine PDAC KPC001 cells (KrasG12D p53R172H/+) were kindly provided by Dr. Yves Boucher (Massachusetts General Hospital, Boston) and were isolated from mice with spontaneous pancreatic tumors (Pdx1Cre/LSL-KrasG12D/p53R172H/+)[2]. Human pancreatic stellate cells (PSCs) were obtained from ScienCell Research Laboratory (California, USA). The human PDAC cell line AsPC-1 was obtained from the American Type Culture Collection (Rockville, MD). AK4.4 cells and KPC001 cells were cultured in high-glucose Dulbecco's modified Eagle's medium (DMEM); PSCs were cultured in RPMI medium with 0.25% stellate cell growth supplement (ScienCell Research Laboratory, California, USA); and AsPC-1 cells were cultured in RPMI medium with 2.5 g/L glucose (A2494001, Thermo Fisher Scientific, USA). All media were supplemented with 10% FBS and 1% penicillin and streptomycin antibiotics (HyClone, Logan, UT). All cells were cultured at 37°C in an incubator (Forma 370, Thermo Fisher Scientific, USA) with an atmosphere of 5% CO₂.

The LQT peptide (NH₂-LQTTCTPHCVSWGGC-COOH) was synthesized and purified (95% purity) by Kelowna International Scientific Inc. (Taipei, Taiwan). Dinitrosyl iron complexes (DNICs) [Fe(μ-SEt)₂(NO)₄] were synthesized according to the reported literature.[3] Poly lactic-coglycolic acid (PLGA, 50/50, inherent viscosity: 0.17 dl/g) was purchased from Green Square Materials Incorporation (Taoyuan, Taiwan). 1,2-Dioleoyl-sn-glycero-3-phosphocholine (DOPC), 1,2-dioleoyl-3-trimethylammonium-propane (DOTAP), 1,2-distearoyl-sn-glycero-3-phosphoethanolamine-N-[methoxy(polyethylene glycol)-2000] (DSPE-PEG(2000)), 1,2-distearoyl-sn-glycero-3-phosphoethanolamine-N-[maleimide(polyethylene glycol)-2000] (DSPE-PEG(2000) maleimide) and cholesterol were purchased from Avanti Polar Lipid (Alabama, USA). Dimethyl sulfoxide (DMSO) and

ethanol (EtOH) were purchased from Sigma-Aldrich (St. Louis, MO). Chloroform, Ni-NTA agarose, and FITC-conjugated albumin from bovine serum (FITC-BSA) were purchased from Thermo Fisher Scientific (USA).

***In vitro-in vivo* combinatorial biopanning of the Ph.D.TM-12 phage display peptide library:**

For *in vivo* phage display selection, a phage library of 10^{11} plaque-forming units (pfu) was intravenously injected into a tumor-bearing mouse and allowed to circulate for 1 hr. Prior to harvest, the mice were sacrificed and perfused with saline to remove the circulating phages. Tumors and other organs were collected and weighed, followed by homogenization (T10 basic, ULTRA-TURRAX, Germany) in 1 mL of RPMI serum-free medium. The homogenized tissues were centrifuged for 10 min at 6000 rpm 4°C and washed with medium 3 times under the same conditions. Afterwards, elution was carried out by adding a 0.5-fold volume to weight ($\mu\text{L}/\text{mg}$) of glycine elution buffer (0.2 M glycine-HCl, pH 2.2) and terminated within 7 min by adding a 15% volume of the elution buffer. The eluate was collected by centrifugation for 10 min at 6000 rpm 4°C and amplified by cultivation with *E. coli* ER2738 shaking at 200 rpm for 4.5 hr at 37°C. After reaching saturation, the *E. coli* was removed by centrifugation at 8000 g for 20 min at 4°C. A 1/6 volume of 20% PEG2000/2.5 M NaCl was subsequently added to the bacteria-free solution to precipitate the phages at 4°C overnight. The precipitated phages were collected via centrifugation at 12000 g 4°C for 20 min, followed by washing with PBS at 10000 rpm for 5 min 4°C. Further purification was performed by precipitation with a 1/6 volume of 20% PEG2000/2.5 M NaCl for 1 hr at 4°C. The amplified phages were obtained by centrifugation at 12000 g 4°C for 15 min with the same washing procedure and were used for subsequent *in vitro* selection with PSCs along with subtraction by FL83B cells. FL83B cells were detached with 10 mM EDTA and counted. A total of 2×10^6 cells were first incubated with 3×10^{10} pfu of selected phages in 1% FBS in PBS at 4°C with shaking for 1 hr. Unbound phages were collected by centrifugation at 2500 rpm and then incubated with 2×10^6 PSCs at 4°C for 2 hr. Unbound phages were washed away 5 times with 0.1% Tween 20 and 1% FBS in PBS at 2500 rpm and 4°C for 1 min each. Elution was then performed by adding glycine elution

buffer and neutralization within 7 min. The recovery process was carried out as described above. All the eluted and recovered phages were titrated on LB/IPTG/Xgal plates using ER2738 culture for subsequent biopanning. The *in vitro* phage display selection was repeated three times to enrich PSC-targeted phages.

Preparation of the Dox-NO@NP formulation:

Dox-NO@NPs were prepared through an oil-in-water single emulsion. PLGA (0.75 mg), DSPE-PEG-maleimide (0.08 mg), D- α -tocopherol polyethylene glycol 1000 succinate (0.375 mg), cholesterol (0.04 mg), DOPC (0.04 mg), Dox (0.05 mg) and DNIC (0.11 mg) were dissolved in 55 μ L of organic phase. The organic phase was added dropwise to 385 μ L of deionized water (volume ratio of oil and water, 1/7) and stirred for 30 mins. The Dox-NO@NPs underwent another 20 cycles of sonication for a total of 1 min 40 s on ice. Each cycle included a 5 s sonication pulse followed by a pulse-off period of 5 s (power, 40 W) with a Q125 sonicator (Qsonica). To obtain Dox-NO@NPs, the emulsion was centrifuged at 25,000 g for 20 min at 25 °C. The resulting pellet of Dox-NO@NPs was resuspended in PBS for further study.

Preparation of the Gem-NO@NP formulation:

Gem-NO@NPs were prepared through an oil-in-water single emulsion. PLGA (0.75 mg), DSPE-PEG-maleimide (0.08 mg), D- α -tocopherol polyethylene glycol 1000 succinate (0.375 mg), cholesterol (0.04 mg), DOPC (0.04 mg), Gem (0.05 mg) and DNIC (0.11 mg) were dissolved in 55 μ L of organic phase. The organic phase was added dropwise to 385 μ L of deionized water (volume ratio of oil and water, 1/7) and stirred for 30 mins. The Gem-NO@NPs underwent another 20 cycles of sonication for a total of 1 min 40 s on ice. Each cycle included a 5 s sonication pulse followed by a pulse-off period of 5 s (power, 40 W) with a Q125 sonicator (Qsonica). To obtain Gem-NO@NPs, the emulsion was centrifuged at 25,000 g for 20 min at 25 °C. The resulting pellet of Gem-NO@NPs was resuspended in PBS for further study.

Tissue distribution of C6-loaded NPs modified with tumor stroma-targeted peptides:

C6 was used as a tracer molecule in the formulation of peptide-modified NPs. FVB/NJNarl female mice with orthotopic implants of AK4.4 cells were injected intravenously with C6-loaded NPs (1.12 mg/kg). Four hours after administration, the mice were sacrificed. The tissues were collected and homogenized in lysis buffer (10 mM Tris-HCl, 1% Triton X-100, 0.1% SDS, 0.1% sodium deoxycholate and 140 mM NaCl). The tissue lysates were kept on ice for 30 min and centrifuged at 16,220 rpm at 4°C for 30 min, and the supernatants were collected.

Animals and orthotopic PDAC models:

FVB/NJNarl female mice C57BL/6 female mice and C. B17/lcr-Prkdc^{scid}/CrINarl female mice were purchased from the National Laboratory Animal Center (Taipei, Taiwan) and BioLASCO Taiwan Company (Taipei, Taiwan). AK4.4 cells (1.0×10^5) were orthotopically implanted into the pancreas of 5- to 6-week-old male FVB mice. KPC001 cells (1.0×10^5) were orthotopically implanted into the pancreas of 5- to 6-week-old male C57 mice and AsPC-1 cells (2.0×10^6) were orthotopically implanted into the pancreas of 5- to 6-week-old male SCID mice. All animals received humane care in compliance with the “Guide for the Care and Use of Laboratory Animals” published by the National Academy of Sciences, and all study procedures and protocols were approved by the Animal Research Committee of National Tsing-Hua University (Hsinchu, Taiwan).

To evaluate anticancer effects in the murine PDAC model, the tumor-bearing mice were randomized into no treatment or treatment groups after tumor implantation. Dox, Gem, TRAIL and DNIC loaded in different formulations (Dox 0.5 mg/kg per dose, Gem 1mg/kg, TRAIL 4 mg/kg per dose, and DNIC 2 mg/kg per dose) were intravenously administered to mice with orthotopic murine PDAC (AK4.4/KPC001) every other day beginning 3 days after implantation. For the orthotopic human PDAC (AsPC-1) tumor xenograft model, TRAIL and DNIC loaded in different formulations (LQT-NO@Nanogel: DNIC 4 mg/kg per dose; LQT-TRAIL@Nanogel: TRAIL 2 mg/kg per dose; LQT-TRAIL-NO@Nanogel: and DNIC 2 mg/kg, TRAIL 1 mg/kg per dose) were intravenously administered

to mice with orthotopic human PDAC (AsPC-1) every other day beginning 3 days after implantation. The tumor volume was evaluated at day 16. The tumor tissue was collected for further analysis.

Tumor perfusion:

Seven days after the implantation of AK4.4 PDAC cells, the mice were treated with LQT-NO@NPs or nontargeted NO@NPs (DNIC: 2 mg/kg) on days 7, 9, 11, 14 and 16; 500 µg of Hoechst 33342 was injected intravenously into the mice 5 min prior to sacrifice on day 17, after which the tumors were harvested. Tumors were embedded in Tissue-Tek (OCT compound) and kept frozen at -80 °C. Tumor tissues were sectioned (10 µm thick) as slides and imaged by confocal microscopy (LSM 780, Zeiss, Germany).

ELISA:

Selected phage clones from the third round of *in vitro* phage display selection were amplified and titrated. PSCs were seeded at a concentration of 8000 cells per well in 96-well plates overnight. The medium was removed, and the cells were washed with PBS and fixed with 4% paraformaldehyde in PBS (100 µL/well) under gentle shaking for 10 min. The cells were then blocked with 280 µL of 1% BSA in PBS in each well for 1 hr. After washing twice with PBS, 10 µL of selected phage clones (8.23×10^{10} pfu/mL) were added along with 40 or 90 µL of PBS and gently shaken for 2 hr. M13KO7 helper phage was used here as control. Unbound phages were removed by washing with PBST (0.5% Tween 20 in PBS) 7 times. HRP/anti-M13 phage primary antibodies (#27942101, GE Healthcare Life Sciences) were added (1:5000 in 1% BSA) and incubated for 1 hr. The same washing procedure was carried out prior to the color change reaction (Reagent A+B) for 6-10 min. The reaction from colorless to blue was terminated by adding stop solution, and the final yellowish solution was analyzed with a UV spectrophotometer (Multiskan, Thermo Scientific, Rockford, IL) at 450 nm. Assay diluent, reagent A&B and stop solution were included in BD OptEIA™ Reagent Set B (BD Bioscience, CA, USA).

Homing:

A total of 10^{11} pfu of selected phage was intravenously injected into AK4.4 orthotopic PDAC tumor-bearing mice 14 days after tumor implantation and allowed to circulate for 1 hr. M13KO7 helper phage was used as control. The phage elution process was performed as described above. The phage eluates from different organs were titrated on LB/IPTG/Xgal plates using ER2738 culture and normalized by weight.

Cellular uptake:

PSCs were seeded at a density of 3×10^4 in 12-well plates with a coverslip in each well and incubated for 24 hr. The unmodified and peptide-decorated NPs containing C6 (0.175 $\mu\text{g}/\text{mL}$) were added for 1 hr. The medium was replaced with 4% paraformaldehyde for 10 min, followed by three washes with PBS. The coverslips containing the cells were mounted with 3 μL of DAPI, fixed on slides, and finally imaged using confocal microscopy (LSM 780, Zeiss, Germany). The images were analyzed using MATLAB.

For the competition assay, the free form of the corresponding peptides and scramble peptide were added to the medium 30 min prior to treatment with the NPs. The cells were incubated with the NPs for another 1 hr.

Immunohistochemistry:

We performed immunostaining for analyzing binding affinity of phages (the LQT28 peptide-displaying M13 phage or the control helper phage) to human pancreatic tumor samples, obtained under the reviewed and approved protocols of the Institutional Review Board of Taipei Veterans General Hospital (IRB2017-01-016C, 2021-07-041BC). The paraffin-embedded tissue blocks were cut into 5- μm -thick tissue sections. Sections were deparaffinized and rehydrated, and antigen retrieval was performed with proteinase K (no. V3021, Promega) for 30 mins at 37°C, followed by incubation with 0.2% Triton® X-100 in PBS for 10 mins. Endogenous peroxidase and nonpecific protein binding were sequentially blocked with 3% H_2O_2 for 30 minutes and 5% bovine serum albumin for 1 hour. Sections were then incubated with the LQT28 peptide-displaying M13 phage or the control helper phage at a concentration of 5×10^{11} pfu/mL at 4°C overnight. After being washed in PBS containing 0.1% Tween

20, sections were incubated with mouse anti-M13 monoclonal antibody(no. AM-D001, Academab Biomedical Inc.) at 1:5000 dilution for 1 hour, which was followed by incubation with Super Enhancer reagent (Super Sensitive Polymer HRP Detection System/DAB, BioGenex) for 20 min and Poly-HRP reagent (BioGenex) for 30 min. After washing, the sections were developed with DAB (3, 3'-diaminobenzidine) Chromogen (BioGenex) supplemented with Stable DAB buffer, and the reaction was terminated by the addition of ddH₂O. For nuclear staining, the slides were immersed in hematoxylin for 5 min, and subsequently mounted with mounting solution to terminate the reaction. All sections were imaged by using a Nikon microscope (Eclipse E800, Tallahassee, FL) and quantified using 5 random fields per section.

For the evaluation of the binding affinity of peptide-displaying M13 phage, images were quantified by measuring DAB staining intensity and normalized with nucleus. The semi-quantitative immunohistochemistry was processed by Fiji to conduct deconvolution and downstream analysis. M13KO7 Helper Phage (control phage) was used as the negative control. According to the fold change of control phage, the intensity of the staining was classified as negative (< 5-fold), low (5-20 fold), or high (> 20-fold).

Human fibrosis PCR arrays:

PSCs were seeded at a density of 10⁶ in 12-well plates after 24 hours of treatment with DNIC (0.5 μM) and TGFβ-1 (0.5 ng/mL, R&D Systems, MN, USA) in serum-free medium. Further validation was performed using RT² Profiler PCR Arrays Human Fibrosis (PAHS-120Z, Qiagen). cDNA samples along with SYBR Green PCR MasterMix were added to wells preloaded with specific primers in the array. PCR was carried out according to the manufacturer's instructions. The data were subsequently analyzed and plotted using online software offered by the manufacturer.

Quantitative real-time PCR:

A total of 10^6 PSCs were seeded in a 12-well plate and treated for 24 hours with DNIC (0.5 μ M) and TGF β -1 (0.5 ng/mL, R&D Systems, MN, USA) in serum-free medium. The cells were washed with ice cold PBS. One microgram of the isolated RNA samples was used to synthesize cDNA using a High-Capacity cDNA Reverse Transcription kit (Applied Biosystems, CA, USA) in a SimpliAmp Thermal Cycler (Thermo Fisher Scientific, MA, USA) following the manufacturer's instructions. Primers specific for *ASMA*, *COL1*, *TGF- β* , *IL1A*, *IL1B*, *IL6*, *IL11*, *CXCL1*, *CXCL2*, *CSF3* and *GAPDH* were used, and relative gene expression was determined using Real-Time SYBR Green PCR Master Mix (Applied Biosystems) on a QPCR System. The comparative threshold cycle method was used to calculate the fold change in gene expression, which was normalized to *GAPDH* as a reference gene. The primer sequences used were as follows.

<i>Gene</i>	<i>Primer Sequences</i>
<i>hASMA</i>	For: 5'-CGTTACTACTGCTGAGCGTGA-3' Rev: 5'-AACGTTCAATTCGGATGGTG-3'
<i>hCOL1</i>	For: 5'-GAACGCGTGTCAATCCCTTGT-3' Rev: 5'-GAACGAGGTAGTCTTTCAGCAACA-3'
<i>hTGF-β</i>	For: 5'-CCCAGCATCTGCAAAGCTC-3' Rev: 5'-GTCAATGTACAGCTGCCGCA-3'
<i>hIL1A</i>	For: 5'-TGTATGTGACTGCCCAAGATGAAG-3' Rev: 5'-AGAGGAGGTTGGTCTCACTACC-3'
<i>hIL1B</i>	For: 5'-AATCTGTACCTGTCCTGCGTGTT-3' Rev: 5'-TGGGTAATTTTTGGGATCTACTACTCT-3'
<i>hIL6</i>	For: 5'-GGTACATCCTCGACGGCATCT-3' Rev: 5'-GTGCCTCTTTGCTGCTTTCAC-3'

<i>hLL11</i>	For: 5'-GGACCACAACCTGGATTCCCTG-3' Rev: 5'-AGTAGGTCCGCTCGCAGCCTT-3'
<i>hCXCL1</i>	For: 5'-AGTGGCACTGCTGCTCCT-3' Rev: 5'-TGGATGTTCTTGGGGTGAAT-3'
<i>hCXCL2</i>	For: 5'-GGCAGAAAGCTTGTCTCAACCC-3' Rev: 5'-CTCCTTCAGGAACAGCCACCAA-3'
<i>hCSF3</i>	For: 5'-ATAGCGGCCTTTTCCTCTACC-3' Rev: 5'-GCCATTCCCAGTTCTTCCAT-3'
<i>hGADPH</i>	For: 5'-AATCCCATCACCATCTTCCA-3' Rev: 5'-TGGACTCCACGACGTACTCA-3'

Coculture system of PDAC tumor cells and PSCs:

For the coculture system, PSCs in the bottom compartment and AsPC-1 cells in the top compartment of 12-well Transwell plates were separated by 0.4 μm inserts (3470, Corning, USA). PSCs were seeded at a density of 2×10^5 in the 12-well plates, and 2×10^5 AsPC-1 cells were seeded on top of the Transwell membrane (0.4 μm pore size). After 24 h of treatment with DNIC (2 μM), PSCs were evaluated by RT-qPCR as described above.

Evaluation of DNIC destruction kinetics:

The DNIC destruction kinetics were investigated at pH 7.4 at 37 $^{\circ}\text{C}$ after loading in NO@nanogel. Briefly, NO@nanogels were suspended in 1 mL of PBS and then incubated at 37 $^{\circ}\text{C}$ in a 100 rpm orbital shaker. At the different time points, 50 μL of solution was harvested, dissolved in 50 μL of DMSO and analyzed by UV spectrophotometry at 360 nm.

Cumulative release of NO:

The release profile of NO from the NO@nanogel was investigated at pH 7.4 at 37 $^{\circ}\text{C}$. Briefly, NO@nanogel (DNIC: 1 mM) was suspended in 1 mL of PBS. DAR-1 (5 μM) was added to the solution and then incubated at 37 $^{\circ}\text{C}$ at 200 rpm in an orbital shaker. At the different time points, 50 μL of solution

was harvested, and the fluorescence intensity (excitation at 566 nm, emission at 596 nm) was measured using a microplate reader (Spark 10M, Tecan).

Cumulative release of protein cargo from the nanogel:

FITC-conjugated BSA was loaded in the nanogel as a model protein. The release profile of FITC-conjugated BSA from the nanogel was investigated at pH 5.5 and 7.4 at 37°C. Briefly, FITC-BSA@nanogel and FITC-BSA-NO@nanogel were suspended in 1 mL PBS buffer or acetic buffer (pH 5.5) and then incubated at 37°C in a 200 rpm orbital shaker. At the different time points, the solution was harvested and centrifuged at 25,001 g for 30 min at 25 °C, and the pellet was resuspended in 200 µL of PBS. The solution was then mixed with the same volume of DMSO, and the fluorescence intensity (excitation at 494 nm, emission at 520 nm) was analyzed by a microplate reader (Spark 10M, Tecan).

Pharmacokinetic study:

FVB/NJNarl female mice were injected intravenously with free-form FITC-labeled TRAIL or FITC-labeled TRAIL loaded in the LQT-TRAIL-NO@Nanogel. At different time points, 200 µL of blood was collected from the orbital sinus and mixed with 20 µL of 0.5 M EDTA. The blood was transferred to a black 96-well plate (Corning). The fluorescence intensity of the sample was measured using a plate reader (Spark 10M, Tecan, Germany) at an excitation wavelength of 494 nm and an emission wavelength of 520 nm. The TRAIL concentration in each sample was calculated from a standard curve.

Apoptosis assay *in vitro*:

AK4.4 or AsPC-1 PDAC cells were seeded at a density of 5×10^5 or 2×10^6 , respectively, in 12-well plates. Sixteen hours after treatment with Dox, Gem, DNIC or TRAIL protein in serum-free medium, the cells were harvested. Further validation was performed using a FITC Annexin V assay (556419, BD Biosciences) and flow cytometry. Flow cytometry data were obtained from a BD FACSAria III flow cytometer (Becton Dickinson) and analyzed with FACSDiva™ software.

TRAIL extraction:

A His₆-tagged human TRAIL expression plasmid (pQE-hTR) that expresses the extracellular portion of human TRAIL (aa95-281) was purchased from Addgene (Plasmid #21811; Cambridge, MA, USA). To generate the His₆-tagged mouse TRAIL expression plasmid, cDNA for the extracellular domain of mouse TRAIL (aa99-291) was amplified by polymerase chain reaction (PCR) and subcloned into the pRSET-A vector (Thermo Fisher Scientific). For the expression of His₆-TRAIL, this plasmid was transformed into *E. coli* BL21 (DE3). Overnight culture was diluted 1:100 in fresh LB medium and incubated at 37°C with shaking at 200 rpm until the OD₆₀₀ reached 0.6–0.8. Expression of His₆-TRAIL was then induced with 0.5 mM IPTG (isopropyl-D-thiogalactopyranoside) and shaken at 200 rpm at 30°C for 3 h. Bacterial pellets were lysed by sonication in sonication buffer (50 mM sodium phosphate, pH 8.0, 300 mM NaCl, 10 mM imidazole, and 10 mM β-mercaptoethanol). Following centrifugation, the supernatant was harvested and incubated with Ni-NTA agarose beads (Qiagen), and His₆-TRAIL was purified using a gravity flow column. After washing with sonication buffer containing 20 mM imidazole, the bound proteins were eluted with the same buffer but containing 250 mM imidazole and dialyzed against PBS with 10 mM β-mercaptoethanol. After dialysis, the protein concentration was determined by spectrophotometry (NanoDrop2000, Thermo Fisher Scientific, USA).

PDAC/PSC spheroid formation:

For spheroid formation, cells (1000 AK4.4 or AsPC-1 PDAC cells mixed with 2000 PSCs/well) were seeded onto a round bottom ultralow attachment 96-well microplate (7007, Corning, USA) and centrifuged at 500 g for 5 min. PDAC/PSC spheroids were cultured in RPMI medium with stellate cell growth supplement (ScienCell Research Laboratory, California, USA) and 10% fetal bovine serum and incubated at 37°C under a humidified atmosphere with 5% CO₂.

To analyze the collagen I distribution, PDAC/PSC spheroids were treated with TRAIL (500 ng/ml) and/or DNIC (0.6 μM) loaded in different formulations. After 48 h of treatment, PDAC/PSC spheroids were first fixed in 4% paraformaldehyde (PFA, in PBS) for 10 mins, followed by incubation with a mixture of methanol and acetone for 10 mins. After washing with PBS, the spheroids were blocked with

5% bovine serum albumin solution for an hour at room temperature and incubated with primary antibodies against Coll (no. 34710, Abcam) at 4 °C overnight. After incubation, the spheroids were washed with PBS and incubated with Alexa Fluor® 488-conjugated anti-rabbit IgG secondary antibodies (Invitrogen, Carlsbad, USA) for an hour at room temperature. Unbound antibodies were washed away with PBS, and the spheroids were counterstained with DAPI (Vector Laboratories, Burlingame, CA). All spheroids were imaged by using a confocal laser scanning microscope (LSM780, Zeiss, Germany) and quantified using 4-15 random fields per treatment group. The expression level was quantified by measuring the area occupied by the staining area of interest normalized by the area of DAPI-stained nuclei as the ratio of green/blue (Alexa Fluor 488/DAPI) relative fluorescence units. The fluorescence intensity was analyzed using ImageJ.

To detect apoptotic cells in PDAC/PSC spheroids, the DeadEnd™ Fluorometric TUNEL System (G3250, Promega, USA) was used according to the manufacturer's recommendations. PDAC/PSC spheroids were first treated with TRAIL (4 µg/mL) and/or DNIC (4.8 µM) loaded in different formulations. After 48 h of treatment, the cell spheroids were fixed in 4% paraformaldehyde (PFA, in PBS) for 30 mins at 4°C, followed by incubation with 0.2% Triton® X-100 in PBS for 5 mins. After washing with PBS, the spheroids were equilibrated with equilibration buffer for 10 mins at room temperature and labeled with TdT reaction mix for 1 h at 37°C in a humidified chamber. After incubation, the reaction was stopped with 2X SSC for 15 mins. Unbound TdT reaction mix was washed away with PBS, and the spheroids were counterstained with DAPI (Vector Laboratories, Burlingame, CA). All spheroids were imaged by using a confocal laser scanning microscope (LSM780, Zeiss, Germany) and quantified using 5-17 random fields per treatment group. The apoptotic index was calculated as the fraction of apoptotic nuclei.

H&E staining

Tumor tissues were cut into small pieces and fixed in 4% paraformaldehyde (PFA, in PBS) overnight before embedded in paraffin wax. The sections were then stained with hematoxylin and eosin (H&E) and observed with a Nikon microscope (Eclipse E800, Tallahassee, FL).

Masson's trichrome staining

Tumor tissues were collected and fixed in 4% paraformaldehyde (PFA, in PBS) overnight before it was embedded in paraffin wax. The sections were then stained with Masson's trichrome according to the manufacturer's instructions (Sigma Aldrich); afterward, they were observed using a Nikon microscope (Eclipse E800, Tallahassee, FL) and quantified using 5 random fields per treatment group. For the evaluation of the collagen expression, collagen area and total tissue area were measured with Fiji and colour deconvolution. Collagen volume fraction (CVF) was quantified by dividing collagen area by the total area. For each group, five replicates were counted and calculated.

Immunostaining:

Tumor tissues were fixed in 4% paraformaldehyde (PFA, in PBS) for 8 hours, followed by incubation in 30% sucrose solution (in PBS) overnight. Then, the tissues were embedded in Tissue-Tek (OCT compound) and kept frozen at -80 °C. Tumor tissues were sectioned (10 µm thick) as slides. Frozen sections were fixed in acetone at -20 °C for 10 minutes and washed with PBS. Then, the sections were blocked with 5% bovine serum albumin solution for an hour at room temperature and incubated with primary antibodies against Coll (no. 34710, Abcam) and α -sma (no. 5694, Abcam) at 4 °C overnight. After incubation, the sections were washed with PBS and incubated with Alexa Fluor® 488-conjugated anti-rabbit IgG secondary antibodies (Invitrogen, Carlsbad, USA) for an hour at room temperature. Unbound antibodies were washed away with PBS, and the sections were counterstained with DAPI (Vector Laboratories, Burlingame, CA). All sections were imaged by using a confocal laser scanning microscope (LSM780, Zeiss, Germany) and quantified using 6-12 random fields per treatment group.

The expression level was quantified by measuring the area occupied by the staining area of interest normalized by the area of DAPI-stained nuclei as the ratio of green/blue (Alexa Fluor 488/DAPI) relative fluorescence units. The fluorescence intensity was analyzed using ImageJ.

Assessment of apoptosis by TUNEL staining:

Frozen sections of tumors were stained by using the DeadEnd™ Fluorometric TUNEL System (G3250, Promega, USA) according to the manufacturer's recommendations. Apoptotic cells were counted in 6-9 randomly selected visual fields for each treatment group. The apoptotic index was calculated as the fraction of apoptotic nuclei.

Western blot analysis:

Cells or tissue was lysed in RIPA lysis buffer for 30 min on ice, and the supernatant was collected after centrifugation at 12,000 rcf. Cell lysates were separated on a 10% acrylamide gel and transferred to a PVDF membrane. Membranes were blocked for 1 hr in 5% skim milk and then incubated overnight with polyclonal antibodies against ColI (no. 34710, Abcam), α -sma (no. 5694, Abcam), Bcl-2 (no. 3498, Cell Signaling Technology), Bcl-xL (no. 2764, Cell Signaling Technology), p53 (no. 2524, Cell Signaling Technology), and β -actin (Sigma clone AC-15, #A5441, lot #122M4782).

Table S1. mRNA expression of a panel of 84 key genes involved in fibrosis in human PSCs 24 h after treatment of DNIC (0.5 μ M) measured by an RT2 Profiler PCR Array. The results are expressed as the fold change relative to the untreated control group (n=2).

<i>Gene symbol</i>	<i>Refseq</i>	<i>Description</i>	<i>Fold Regulation</i>
<i>Pro-fibrotic</i>			
ACTA2	NM_001613	Actin, alpha 2, smooth muscle, aorta	-1.4847
CCL11	NM_002986	Chemokine (C-C motif) ligand 11	-1.2484
CCL3	NM_002983	Chemokine (C-C motif) ligand 3	-1.2484
CTGF	NM_001901	Connective tissue growth factor	1.0458
GREM1	NM_013372	Gremlin 1	1.5918
IL13	NM_002188	Interleukin 13	-1.2484
IL13RA2	NM_000640	Interleukin 13 receptor, alpha 2	-1.2484
IL4	NM_000589	Interleukin 4	-1.2484
IL5	NM_000879	Interleukin 5 (colony-stimulating factor, eosinophil)	-1.2484
SNAI1	NM_005985	Snail homolog 1 (Drosophila)	-4.0097
<i>ECM</i>			
COL1A2	NM_000089	Collagen, type I, alpha 2	-1.7548
COL3A1	NM_000090	Collagen, type III, alpha 1	-1.3943
ITGA1	NM_181501	Integrin, alpha 1	-1.136
ITGA2	NM_002203	Integrin, alpha 2 (CD49B, alpha 2 subunit of VLA-2 receptor)	-1.1418
ITGA3	NM_002204	Integrin, alpha 3 (antigen CD49C, alpha 3 subunit of VLA-3 receptor)	-1.2325
ITGAV	NM_002210	Integrin, alpha V (vitronectin receptor, alpha polypeptide, antigen CD51)	-1.3303
ITGB1	NM_002211	Integrin, beta 1 (fibronectin receptor, beta polypeptide, antigen CD29 includes MDF2, MSK12)	-1.0212
ITGB3	NM_000212	Integrin, beta 3 (platelet glycoprotein IIIa, antigen CD61)	-1.5286
ITGB5	NM_002213	Integrin, beta 5	1.1828
ITGB6	NM_000888	Integrin, beta 6	-1.2484
ITGB8	NM_002214	Integrin, beta 8	-1.8697
<i>Remodeling</i>			
LOX	NM_002317	Lysyl oxidase	-1.1218
MMP1	NM_002421	Matrix metalloproteinase 1 (interstitial collagenase)	-1.7868
MMP13	NM_002427	Matrix metalloproteinase 13 (collagenase 3)	-1.2484
MMP14	NM_004995	Matrix metalloproteinase 14 (membrane-inserted)	-1.4263
MMP8	NM_002424	Matrix metalloproteinase 8 (neutrophil collagenase)	-1.2484
PLAT	NM_000930	Plasminogen activator, tissue	1.061
PLAU	NM_002658	Plasminogen activator, urokinase	-1.6357
PLG	NM_000301	Plasminogen	-1.2484
SERPINA1	NM_000295	Serpin peptidase inhibitor, clade A (alpha-1 antiproteinase, antitrypsin), member 1	-1.2484
SERPINH1	NM_001235	Serpin peptidase inhibitor, clade H (heat shock protein 47), member 1, (collagen binding protein 1)	-1.0856
TIMP1	NM_003254	TIMP metalloproteinase inhibitor 1	-1.1414
TIMP2	NM_003255	TIMP metalloproteinase inhibitor 2	-1.1051
TIMP3	NM_000362	TIMP metalloproteinase inhibitor 3	-1.2484
TIMP4	NM_003256	TIMP metalloproteinase inhibitor 4	-1.3259
<i>TGFβ</i>			

BMP7	NM_001719	Bone morphogenetic protein 7	-1.2484
CAV1	NM_001753	Caveolin 1, caveolae protein, 22kDa	-1.3078
DCN	NM_001920	Decorin	-1.306
ENG	NM_000118	Endoglin	-1.034
INHBE	NM_031479	inhibin, beta E	-1.8157
LTBP1	NM_000627	Latent transforming growth factor beta binding protein 1	-1.4918
SMAD2	NM_005901	SMAD family member 2	1.3185
SMAD3	NM_005902	SMAD family member 3	-1.1025
SMAD4	NM_005359	SMAD family member 4	1.0312
SMAD6	NM_005585	SMAD family member 6	-1.285
SMAD7	NM_005904	SMAD family member 7	1.1205
TGFB1	NM_000660	Transforming growth factor, beta 1	-1.3694
TGFB2	NM_003238	Transforming growth factor, beta 2	-1.2207
TGFBR1	NM_004612	Transforming growth factor, beta receptor 1	1.3015
TGFBR2	NM_003242	Transforming growth factor, beta receptor II (70/80kDa)	1.0197
TGIF1	NM_003244	TGFB-induced factor homeobox 1	-1.0644
THBS1	NM_003246	Thrombospondin 1	1.0442
THBS2	NM_003247	Thrombospondin 2	-1.9603

Growth Factors

AGT	NM_000029	Angiotensinogen (serpin peptidase inhibitor, clade A, member 8)	-1.1219
EDN1	NM_001955	Endothelin 1	1.0081
EGF	NM_001963	Epidermal growth factor	-1.2484
HGF	NM_000601	Hepatocyte growth factor (hepapoietin A; scatter factor)	-1.526
PDGFA	NM_002607	Platelet-derived growth factor alpha polypeptide	-1.2879
PDGFB	NM_002608	Platelet-derived growth factor beta polypeptide	-1.2484
VEGFA	NM_003376	Vascular endothelial growth factor A	-1.1115

Transcription Factors

CEBPB	NM_005194	CCAAT/enhancer binding protein (C/EBP), beta	-1.2311
JUN	NM_002228	Jun proto-oncogene	-1.0197
MYC	NM_002467	V-myc myelocytomatosis viral oncogene homolog (avian)	1.0115
NFKB1	NM_003998	Nuclear factor of kappa light polypeptide gene enhancer in B-cells 1	1.1326
SP1	NM_138473	Sp1 transcription factor	-1.4095
STAT1	NM_007315	Signal transducer and activator of transcription 1, 91kDa	-1.0492
STAT6	NM_003153	Signal transducer and activator of transcription 6, interleukin-4 induced	1.4406

Inflammatory Cytokines & Chemokines

CCL2	NM_002982	Chemokine (C-C motif) ligand 2	-1.1603
CCR2	NM_001123396	Chemokine (C-C motif) receptor 2	-3.6378
CXCR4	NM_003467	Chemokine (C-X-C motif) receptor 4	-1.2484
IFNG	NM_000619	Interferon, gamma	-1.2484
IL10	NM_000572	Interleukin 10	-1.2484
IL1A	NM_000575	Interleukin 1, alpha	-1.2484
IL1B	NM_000576	Interleukin 1, beta	-1.2484
TNF	NM_000594	Tumor necrosis factor	-1.2484

EMT

AKT1	NM_005163	V-akt murine thymoma viral oncogene homolog 1	-1.2348
ILK	NM_004517	Integrin-linked kinase	-1.1855
MMP2	NM_004530	Matrix metalloproteinase 2 (gelatinase A, 72kDa gelatinase, 72kDa type IV collagenase)	-1.4007
MMP3	NM_002422	Matrix metalloproteinase 3 (stromelysin 1, progelatinase)	1.8034

MMP9	NM_004994	Matrix metalloproteinase 9 (gelatinase B, 92kDa gelatinase, 92kDa type IV collagenase)	-1.1422
SERPINE1	NM_000602	Serpin peptidase inhibitor, clade E (nexin, plasminogen activator inhibitor type 1), member 1	1.1381
TGFB3	NM_003239	Transforming growth factor, beta 3	1.5498
<i>Other Fibrosis Genes</i>			
BCL2	NM_000633	B-cell CLL/lymphoma 2	-1.2484
FASLG	NM_000639	Fas ligand (TNF superfamily, member 6)	-1.2484
<i>Host Gene</i>			
ACTB	NM_001101	Actin, beta	-1.0372
B2M	NM_004048	Beta-2-microglobulin	1.1221
GAPDH	NM_002046	Glyceraldehyde-3-phosphate dehydrogenase	-1.1274
HPRT1	NM_000194	Hypoxanthine phosphoribosyltransferase 1	1.2952
RPLP0	NM_001002	Ribosomal protein, large, P0	-1.2428

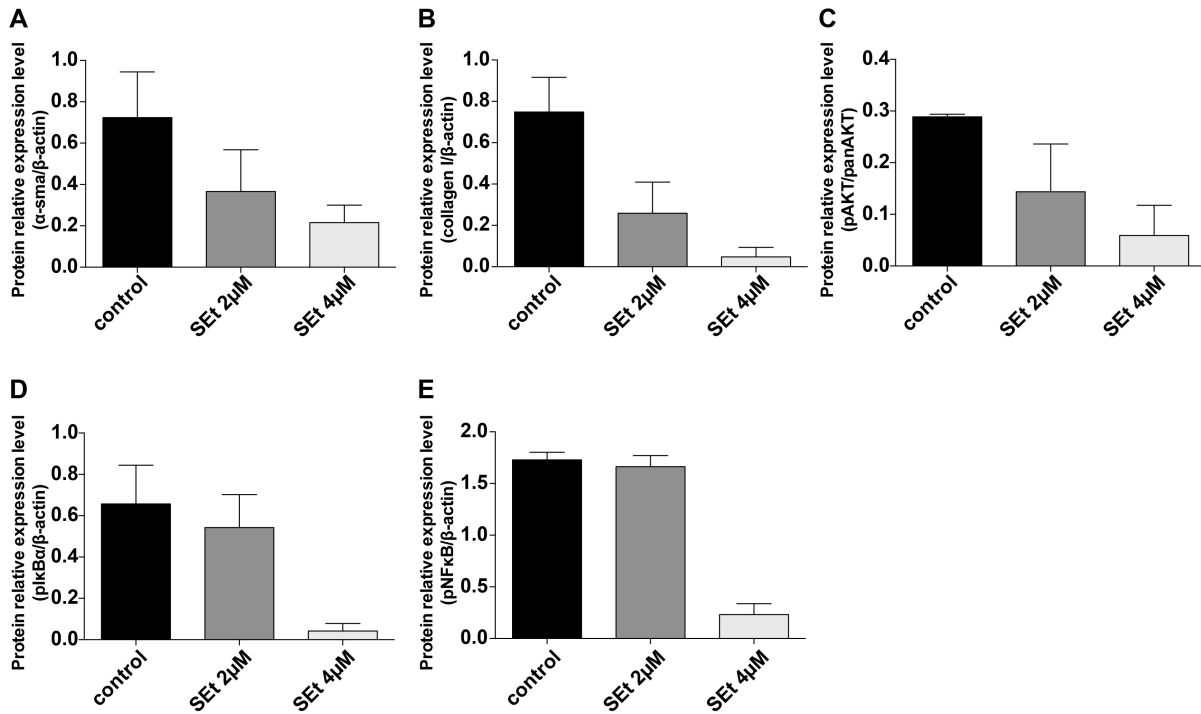


Figure S1. Western blot quantification of fibrosis-related protein by ImageJ. Western blotting was used to analyze α -SMA and collagen I protein expression as well as downstream TGF β signaling activation (phospho-AKT, phospho-NF- κ B and phospho-I κ B α levels) in primary, culture-activated human PSCs treated with or without increasing concentrations of DNIC. The band intensity of protein was normalized by β -actin or panAKT of the same sample (n=2).

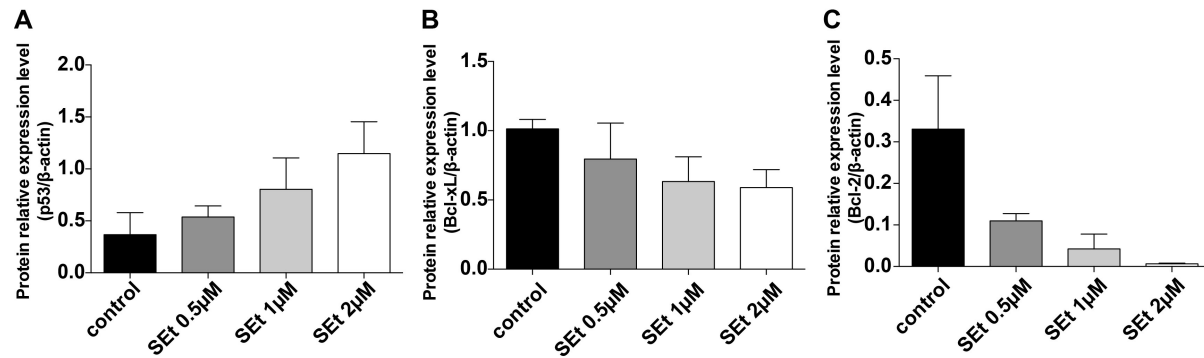


Figure S2. Western blot quantification of apoptosis-related protein by ImageJ. Western blotting was used to analyze p53, Bcl-xL and Bcl-2 expression in AK4.4 cells. The band intensity of protein was normalized by β -actin of the same sample (n=2).

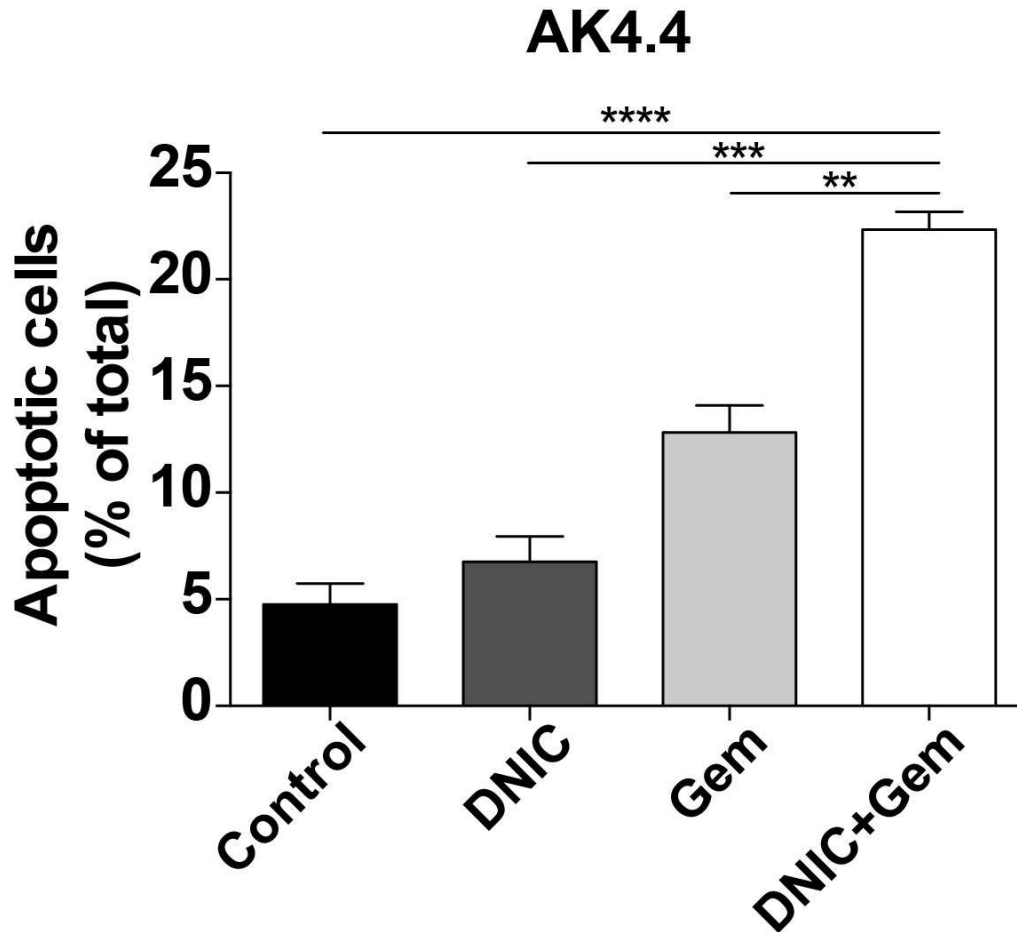


Figure S3. The impact of NO on Gem-induced anticancer effects. Gem (2 μ M) in combination with DNIC (2 μ M) significantly enhanced the induction of apoptosis in murine AK4.4 PDAC cells, as detected using annexin V staining (n=3-4). All data are shown as the mean \pm s.e.m. ** P <0.01, *** P <0.001, **** P <0.0001.

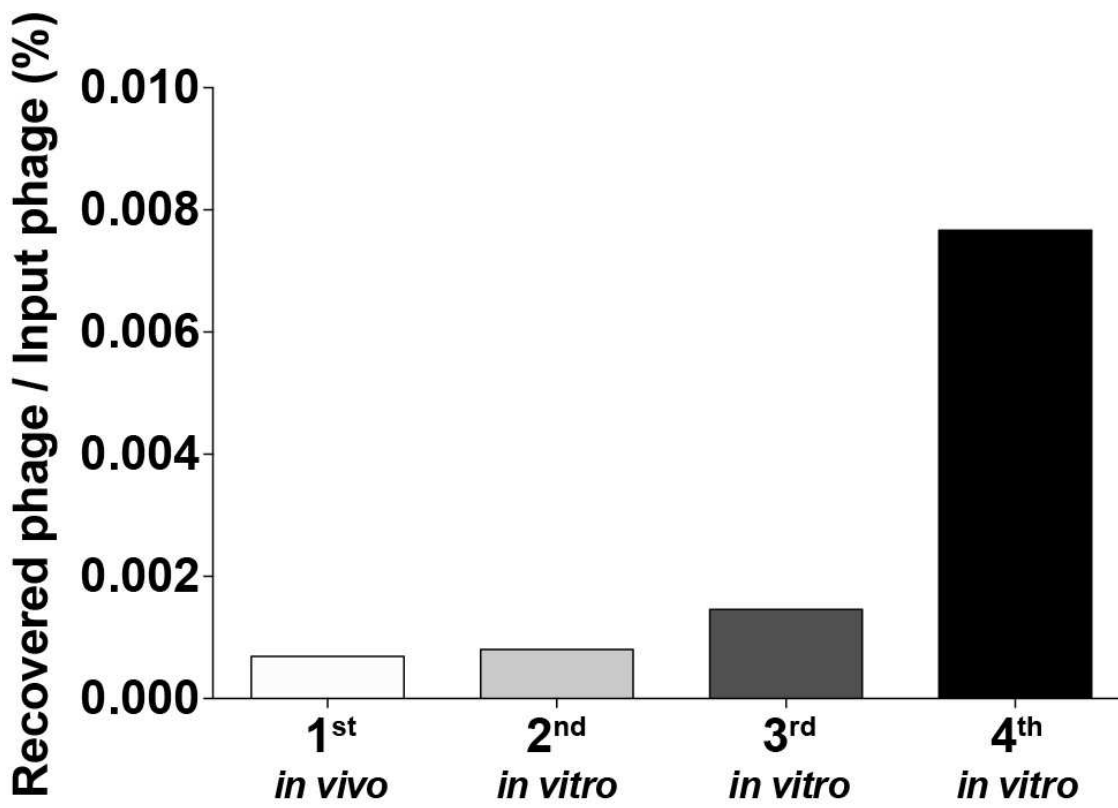


Figure S4. Phage titer after each round of biopanning. The eluted M13 phage titer percentage compared to the input titer from each round of biopanning.

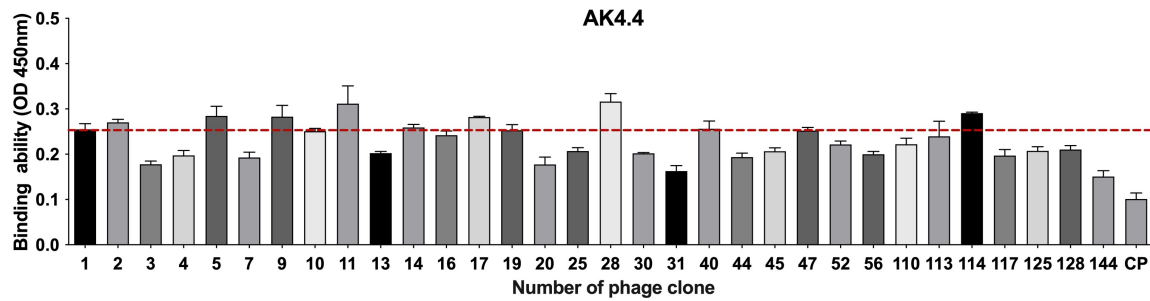


Figure S5. ELISA of the selected phage clones binding to the murine PDAC AK4.4 cells. The murine PDAC AK4.4 cells were incubated with representative phage clones expressing different sequences (n=3). A control phage without an insert was used as the negative control. The red line indicates a threshold binding affinity >2.5-fold greater than that of the negative control helper phage threshold.

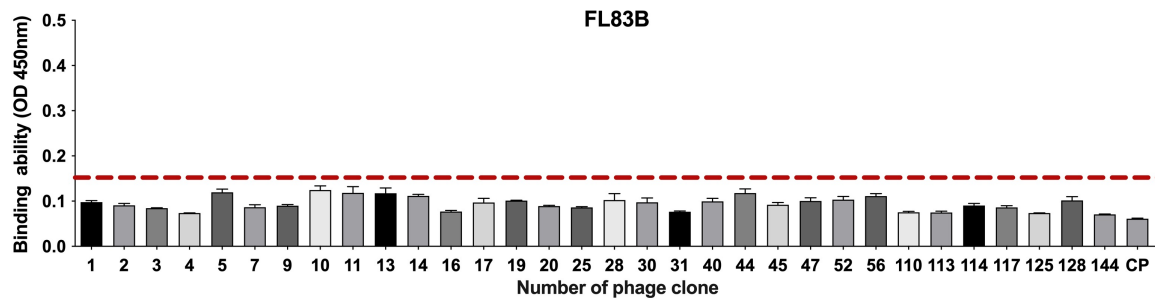


Figure S6. ELISA of the selected phage clones binding to the normal hepatocytes (FL83B). The normal hepatocytes (FL83B) were incubated with representative phage clones expressing different sequences (n=3). A control phage without an insert was used as the negative control. The red line indicates a threshold binding affinity >2.5-fold greater than that of the negative control helper phage threshold.

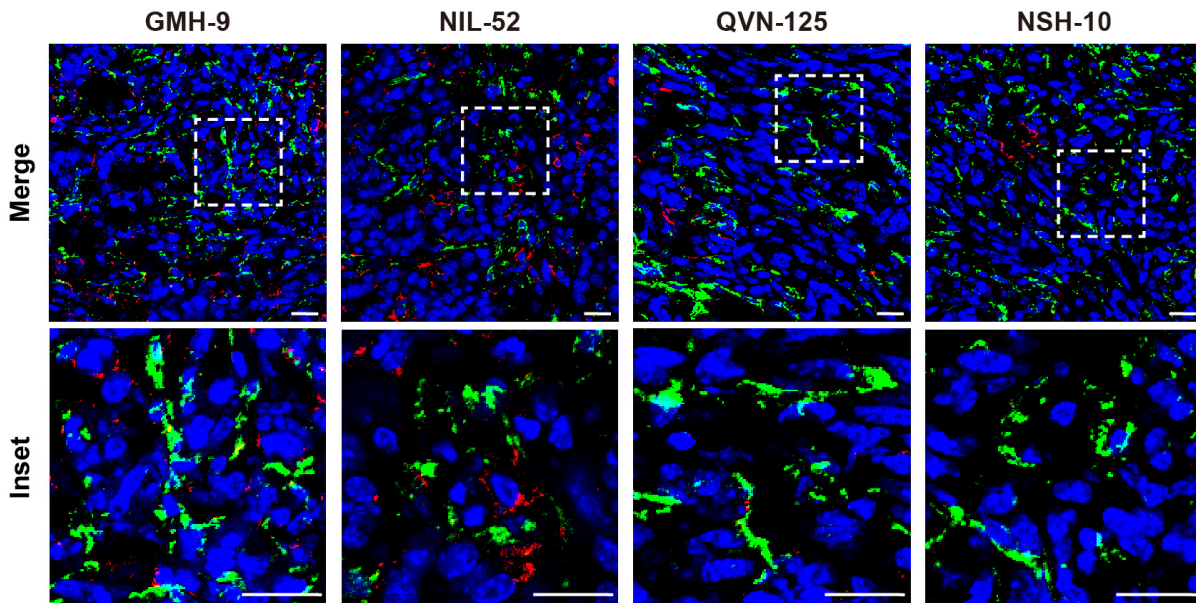


Figure S7. Representative images of immunofluorescence (IF) staining to detect phage clones in

PDAC. Red, phage (anti-M13 antibody); green, α -SMA; blue, nuclei (DAPI). Scale bars, 20 μ m.

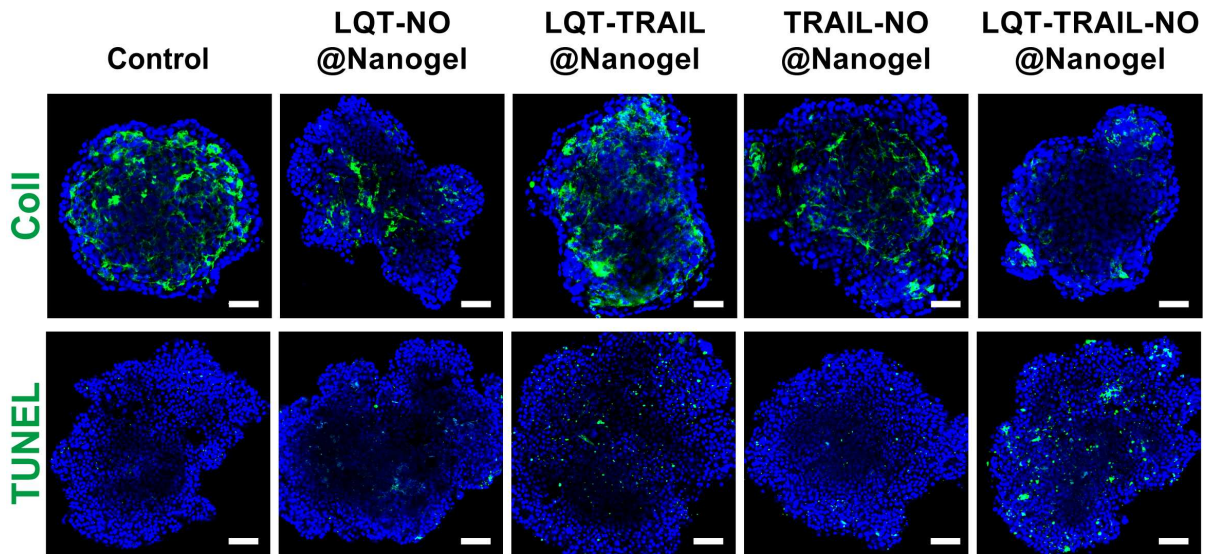


Figure S8. Representative immunofluorescence images of AK4.4 PDAC cell/PSC 3D spheroid cultures after treatment with different formulations. Green, collagen I or TUNEL staining; blue, nuclei (DAPI). Scale bars, 50 μ m.

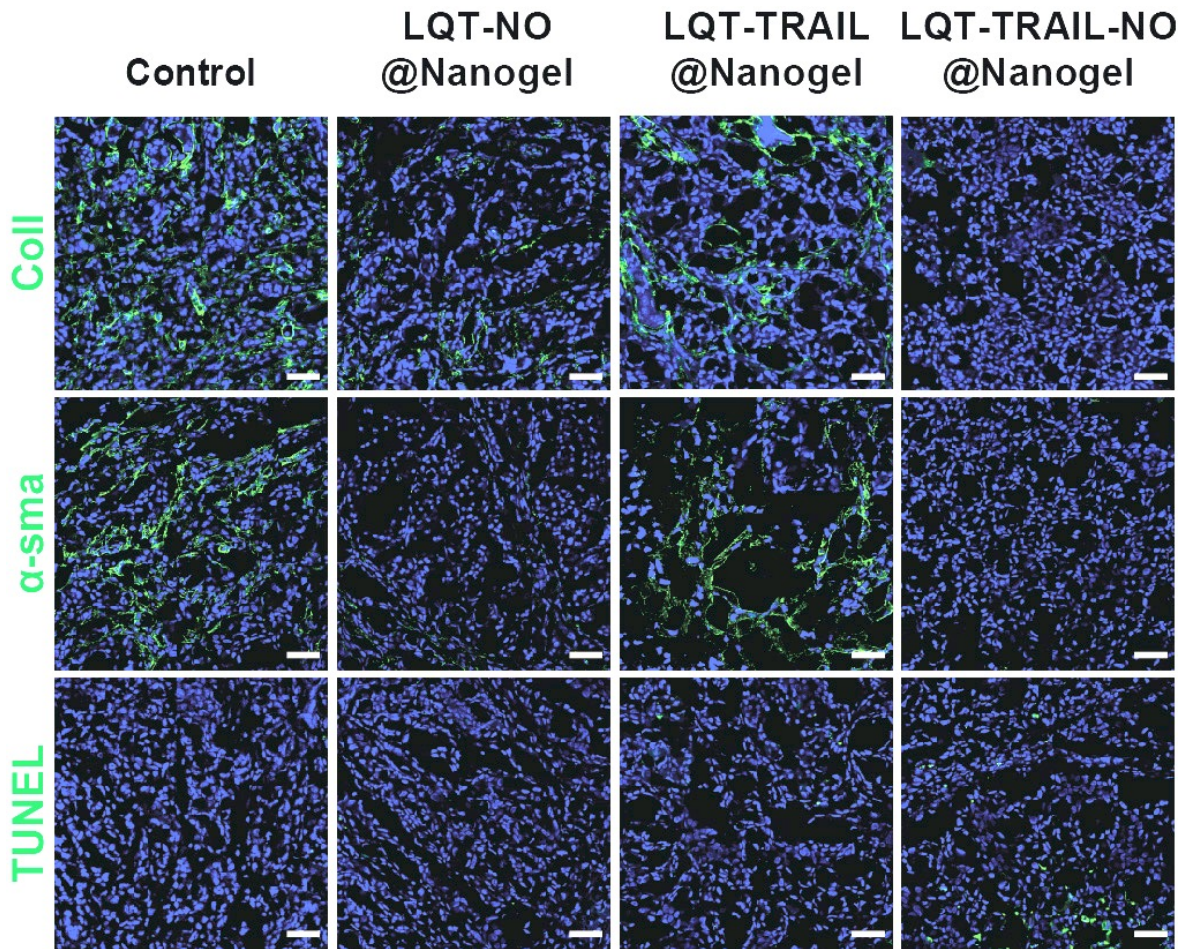


Figure S9. Representative immunofluorescence images of collagen I, α -SMA and TUNEL staining in tumors of orthotopic human PDAC (AsPC-1) models after treatment of various formulations. Scale bar, 50 μ m.

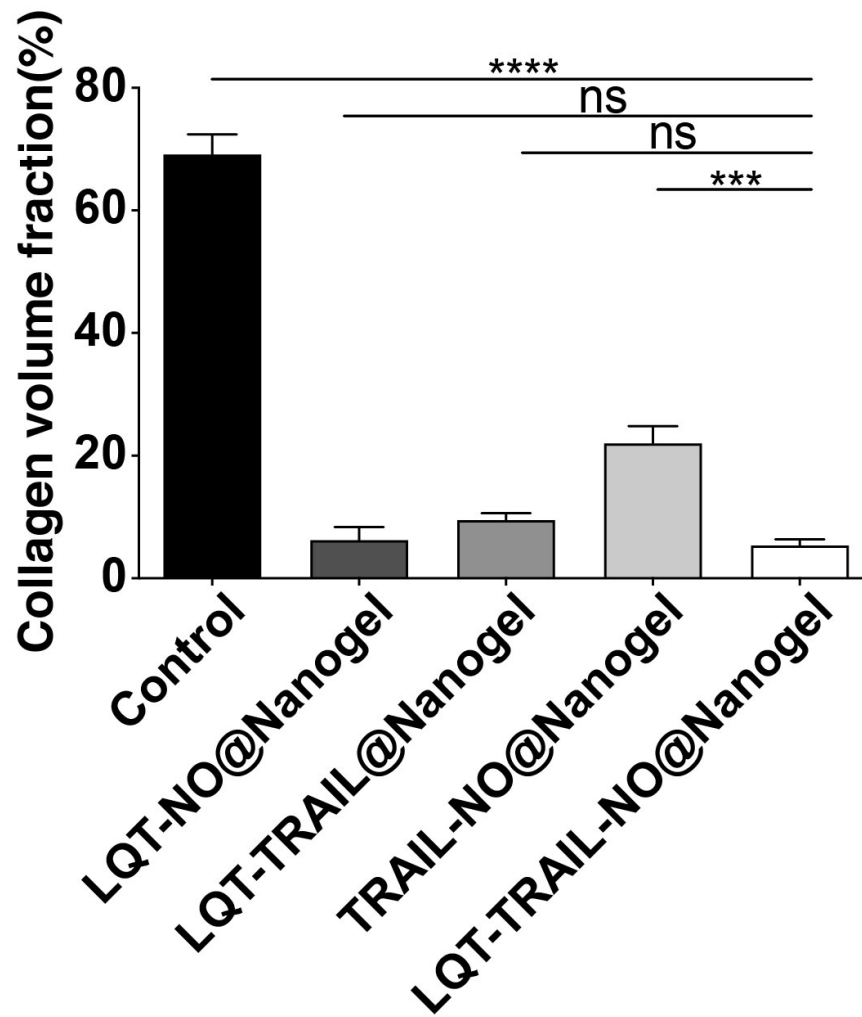


Figure S10. Masson's trichrome staining quantification in nanogel-treated murine AK4.4 PDAC. Delivery of TRAIL and NO by tumor stroma-targeted nanogels reduced collagen production in murine AK4.4 PDAC. The images were analyzed by Masson's trichrome staining and quantified by Fiji(n=5). All data are shown as the mean \pm s.e.m. *** P <0.001, **** P <0.0001.

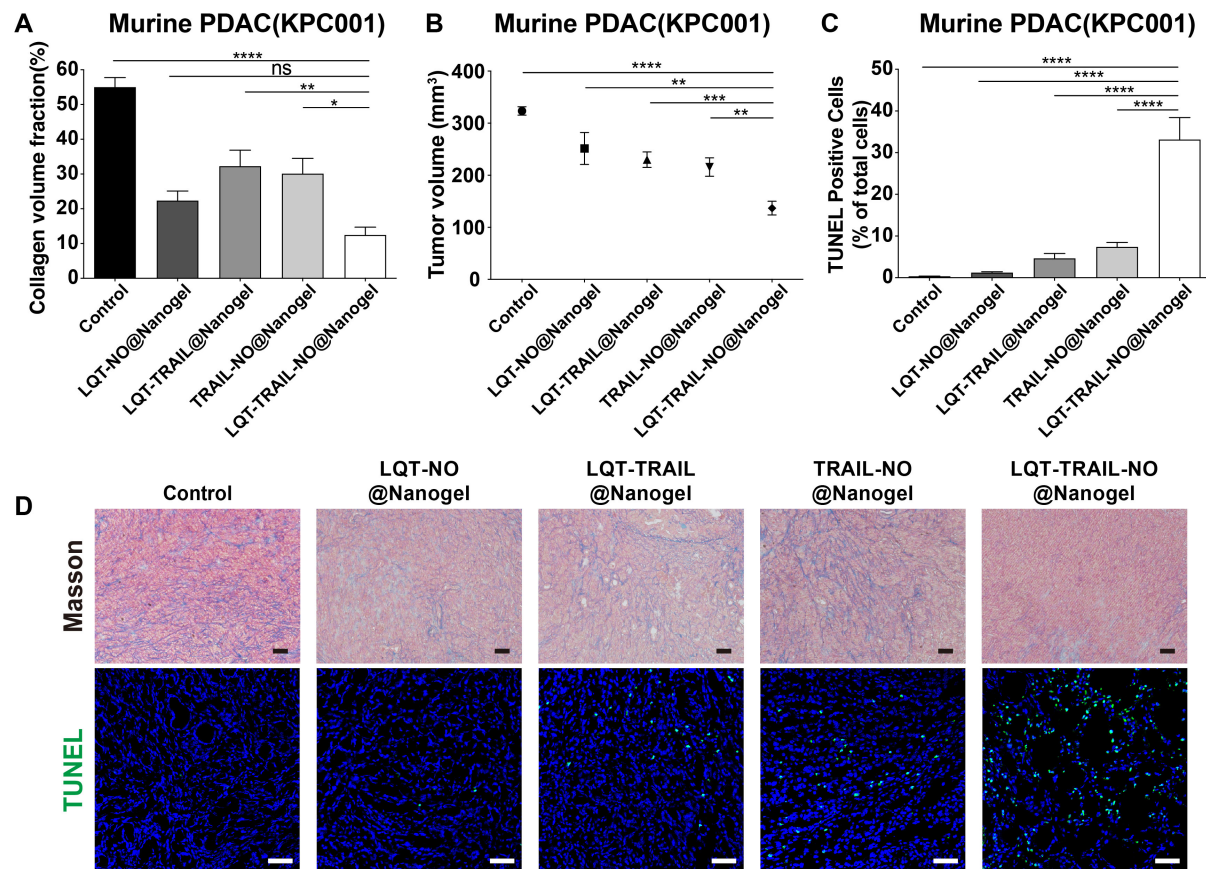


Figure S11. Delivery of TRAIL and NO by tumor stroma-targeted nanogels reduced collagen production, increased apoptosis induction and suppressed tumor growth in murine orthotopic KPC001 PDAC models. (A) LQT-TRAIL-NO@Nanogel significantly reduced collagen production was analyzed by Masson's trichrome staining. The images were quantified by Fiji (n=5). (B) Volumes of orthotopic KPC001 PDAC tumors 16 days after implantation in treated and untreated (control) mice (n=5-7). (C) LQT-TRAIL-NO@Nanogel significantly enhanced the induction of apoptosis in orthotopic PDAC tumors, as indicated by TUNEL staining (n=7). (D) Representative Masson's trichrome staining images showing the results of collagen and TUNEL staining in orthotopic murine PDAC (KPC001) tumors after treatment with various formulations. Blue, nuclei (DAPI). Scale bars, 50 μ m. All data are shown as the mean \pm s.e.m. * P <0.05, ** P <0.01, *** P <0.001, **** P <0.0001.

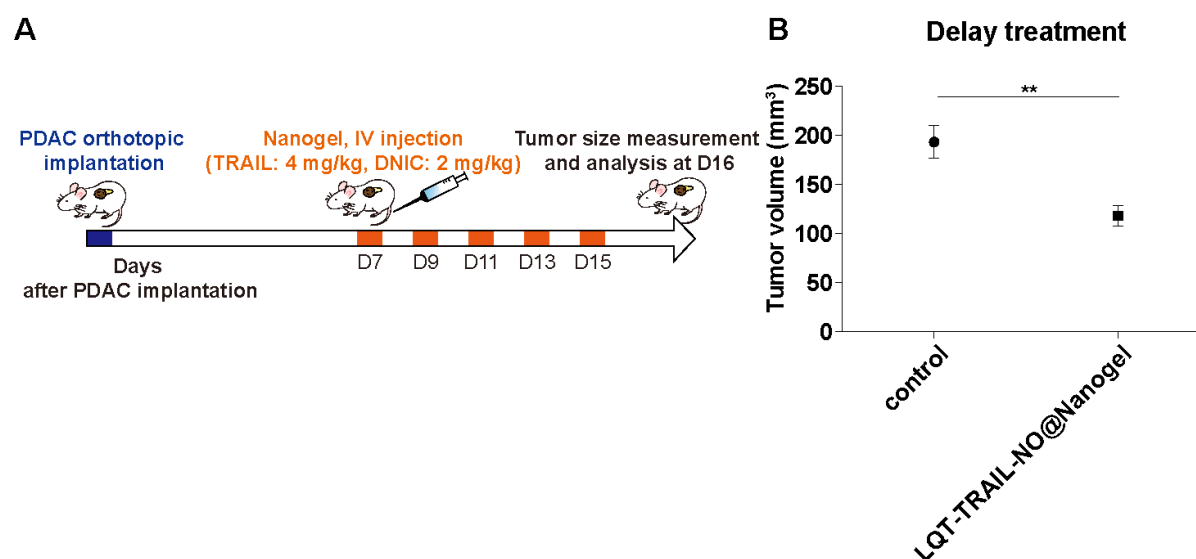


Figure S12. Delayed treatment of TRAIL and NO in tumor stroma-targeted nanogels suppressed tumor growth in murine orthotopic AK4.4 PDAC models. (A) Schematic illustration of delayed LQT-TRAIL-NO@Nanogel treatment protocol. After the implantation of PDAC cells, mice were treated intravenously with various NP formulations encapsulating the NO donor DNIC and/or TRAIL on days 7, 9, 11, 13 and 15; tumor volume was measured on day 16. (B) Volumes of orthotopic PDAC tumors 16 days after implantation in treated and untreated (control) mice (n=7).

Reference:

- 1 Bardeesy N, Cheng KH, Berger JH, Chu GC, Pahler J, Olson P, *et al.* Smad4 is dispensable for normal pancreas development yet critical in progression and tumor biology of pancreas cancer. *Genes Dev* 2006;**20**:3130-46.
- 2 Sharma NS, Gupta VK, Garrido VT, Hadad R, Durden BC, Kesh K, *et al.* Targeting tumor-intrinsic hexosamine biosynthesis sensitizes pancreatic cancer to anti-PD1 therapy. *J Clin Invest* 2020;**130**:451-65.
- 3 Lu TT, Tsou CC, Huang HW, Hsu IJ, Chen JM, Kuo TS, *et al.* Anionic Roussin's red esters (RREs) syn-/anti-[Fe(μ -SEt)(NO)₂]₂(-): the critical role of thiolate ligands in regulating the transformation of RREs into dinitrosyl iron complexes and the anionic RREs. *Inorg Chem* 2008;**47**:6040-50.